

Use of a high-resolution pore-water gel profiler to measure groundwater fluxes at an underwater saline seepage site in Lake Kinneret, Israel

Abstract—We have used new gel pore-water profilers and conventional seepage meters to determine the advective flux of water from an underwater saline seep into Lake Kinneret. The gel probes sampled pore waters from medium to coarse sands that could not be sampled by conventional coring methods. The anions Cl, Br, and SO₄ were constant at levels just above those for the lake for 3–5 cm into the sediment due to wave action or other turbulent mixing processes. There was then a sharp increase in concentration to values of approximately 8,000 mg Cl liter⁻¹, 370 mg SO₄ liter⁻¹, and 120 mg Br liter⁻¹ at a depth of ~8.5 cm. Using an advection–diffusion model, the linear interstitial advection velocity (LIV) of the groundwater into the lake was calculated to vary between 140 and 275 cm yr⁻¹. The LIV values from conventional seepage flux meters at the same site were 30 and 164 cm yr⁻¹. Differences between the LIV measurements of these two methods may be due to a number of possible factors, including groundwater flux heterogeneity.

Groundwater seepage directly into lakes can be an important process both as it affects the overall water budget and in many situations the water quality of the lake (see Boyle [1994] and references therein). The flux of saline water from seepage into a lake can be estimated from detailed pore-water chemical profiles using an advection–diffusion model (Munk 1966; Berner 1972; Lee et al. 1980; Cornett et al. 1989). A requirement of such studies is that it is possible to determine a pore-water profile of sufficient resolution to resolve different solutions of the model. In this study, we have used a recently developed technique employing gel sampler probes (Krom et al. 1994; Mortimer et al. 1998). Previous attempts to sample pore waters at these sublittoral sites have not been successful because conventional sediment corers, whether deployed from a boat or by a diver, tend to bounce off the sandy substrate or the corers do not hold the sediment. We have measured high-resolution pore-water profiles of chloride, bromide, and sulfate at three locations in the area of the saline seeps offshore from the Tiberias hot springs and then modeled the resulting profiles to estimate the flux of saline water into Lake Kinneret.

The seepage rate of groundwater into a lake can also be measured directly using seepage meters. Several designs have been proposed (e.g., Lee 1977; Cherkauer and McBride 1988; Boyle 1994). It has been shown that the most reliable and cost-effective seepage meter design employs an inverted container with a seepage bag mounted on its top to measure water displacement over a specified area of the lake bottom (Lee 1977; Lee and Cherry 1978; Boyle 1994). In the Kinneret study we have used a modified seepage meter designed by Boyle (1994) to measure the groundwater seepage rate directly. The seepage rates measured by the seepage meter were compared with flux rates estimated from modeling the pore-water profiles measured using the gel probes.

The primary purpose of this research was to make an initial assessment of the compatibility, reproducibility, and installation logistics of these two methods with the aim of providing better estimates of littoral groundwater discharge into lakes.

Lake Kinneret serves as a major source (~30%) of drinking and irrigation water to Israel. The principal source of freshwater into Lake Kinneret is the inflowing Jordan River with a chlorinity of 17 mg Cl liter⁻¹. There are a number of onshore saline springs that discharged into the lake and were diverted in 1964 into a channel. As a result, the salinity of the lake decreased from 365 mg Cl liter⁻¹ in 1964 to its present level of 225 ± 30 mg Cl liter⁻¹ (Nishri et al. 1999). The present salinity balance indicates that there are substantial internal salinity sources to the lake estimated to be 90,000 tones of chloride per year (Smith et al. 1989). A number of point sources of saline groundwater have been identified on the lake bottom (e.g., Tabgha and Fulya areas). However, there have been no studies that quantify the flux of saline water from these subaqueous springs. Recently, an area of saline seeps has been located offshore of the Tiberias Hot Springs (THS) (Manwaring 1996); springs that have been used for therapeutic and recreational purposes since at least Roman times. It was an aim of this study to determine the flux of saline water from these potentially important seepage areas into the lake.

Protocol—Pore waters at three sites were sampled using gel probes. The sites were situated at 30 m (Sta. 30), 35 m (Sta. 35), and 37 m (Sta. 37) offshore from the THS in water depths of 4.5, 5.0, and 5.5 m, respectively. The sampling was carried out on 20–21 November 1996. Seepage flux meters were deployed at the first two of these sites, 30 m and 35 m from the 23rd of October 1996 for 1 week. In addition, a sample of water from the THS was collected for chemical comparisons with the pore-water samples.

Gel sampling of the pore waters was performed using the procedure described by Krom et al. (1994). Probe lengths used in this investigation were 40 cm; but it was only possible to insert the probes ~20 cm into the sand because a hard layer was encountered at this depth. The polyacrylamide gels were prepared in Leeds, UK, transported to Israel in watertight plastic containers with Milli-Q water, and assembled a few days before use. The probes were placed directly into the sediment by divers, left to equilibrate overnight, and recovered the next day. The gel was divided immediately after recovery into narrow sections (~0.5 cm), put into tightly closed microcentrifuge tubes, and weighed. Analysis was performed within 1 week using a Dionex ion chromatograph with an autosampler attached.

Replicate analysis of known standards was 1.3% (Cl⁻), 2.9% (Br⁻), and 4.6% (SO₄²⁻; relative standard deviation,

Table 1. Parameters used in Eq. 1 to calculate best-fit curves to the measured pore-water profile.

Station Anion	Linear interstitial velocity	Surface layer concentration: depth of constant concentration from surface*	Constant concentration at depth (C_a in mg L^{-1})	Depth to top of high constant concentration (cms)
30 Cl	275	250:4.5	9,400	9.0
30 Br	275	2:4.5	135	9.0
30 SO_4	275	50:4.5	380	9.0
35 Cl	140	370:3	7,950	8.5
35 Br	140	5:3	109	8.5
35 SO_4	140	55:3	370	8.5
37 Cl	200	450:3.5	8,400	10.0
37 Br	200	5:3.5	115	10.0
37 SO_4	200	75:3.5	350	10.0

* Surface layer concentration refers to C_o in mg L^{-1} ; depth of constant concentration from surface measured in centimeters.

1s, $n = 12$). Total precision (1s), determined by analyzing five replicate samples of anion gel taken from several centimeters above the benthic boundary, was 2.5% (Cl^-) and 3.8% (SO_4^{2-} ; Krom et al. 1994). At the same time the sample of water from THS was determined after dilution by a factor of 40 to bring the sample within analytical range.

Seepage flux meters were constructed following the design given in Boyle (1994). The seepage collector component of the meter is a large inverted, round plastic container with a cross-sectional area of 0.322 m^2 . It is gently worked into the lake sediment by a diver until it is well seated (generally 5–10 cm) and then stabilized on the lake floor by a surrounding perforated tubular collar filled with sand. After the diver has placed the collector component on the sediment surface it is allowed to stabilize for several days. A 7-liter seepage sampling bag was filled with exactly 1 liter of water colored with red food dye to aid visual observation during sampling and seepage volume measurement. The sampling bag and a protective pail used to protect it from wave action (artificial pumping) and nibbling fish were then lowered into the water and connected to the seepage collector as described in Boyle (1994). At the end of the collection period (7 d), the seepage bag was closed off and disconnected from the collector and the volume of water in it was measured (after subtracting the initial bag volume of 1 liter). The seepage flux from the sediment into the lake ($\text{liters m}^{-2} \text{ d}^{-1}$) was calculated by dividing the net volume collected (liters) by the seepage collector area (0.322 m^2) and the period of collection (7 d). The macroscopic seepage flux (MSF, cm yr^{-1}) at the sediment–water interface can be calculated by multiplying the measured seepage flux ($\text{liters m}^{-2} \text{ d}^{-1}$) by 36.5 ($1,000 \text{ cm}^3 \times 365 \text{ d}/10^4 \text{ cm}^2$). The linear advection velocity within the sediment (LIV) is then calculated by dividing the MSF by the sediment porosity.

Lee (1977), Erickson (1981), and Cherkauer and McBride (1988) have all noted a drop in the ability of their meters to measure true seepage fluxes when tested using laboratory tank studies. This drop in efficiency that can be between 15 and 40% is largely a factor of design features of the meter that cause resistance to fluid flow and the lack of proper equilibration time of the meter in the lake sediments before arming with a seepage bag. Lee (1977) has also noted that silt sedimentation, after disturbance during installation of the

meter, may also cause reductions in efficiency. The use of an equilibration time before arming with a seepage bag and a premeasured amount of water in the bag, shown by Erickson (1981) to increase efficiency, suggest that the efficiency for the present system is on the order of 80%. In the absence of a measured efficiency factor for the meter system, the measured seepage fluxes obtained should be considered minimum values.

Pore-water profiles and seepage flux data obtained—The chloride concentration at Sta. 35 was almost constant at a value of $370 \text{ mg Cl liter}^{-1}$ from 1.5 cm above the sediment–water interface to a depth of 3 cm into the sediment (Fig. 1; Table 1). Below 3 cm there was a sharp increase in pore-water chloride concentration reaching a value of $7,950 \text{ mg Cl liter}^{-1}$ at 8.5 cm and then remaining constant to the bottom of the sediment profile (12.5 cm). The pore-water profiles of sulfate and bromide were similar in shape to that of chloride with constant values of $\sim 5 \text{ mg Br liter}^{-1}$ and $\sim 55 \text{ mg SO}_4 \text{ liter}^{-1}$ to a depth of 2.5 cm, a sharp increase to values of $109 \text{ mg Br liter}^{-1}$, and $370 \text{ mg SO}_4 \text{ liter}^{-1}$ at a depth of 8.5 cm, and constant concentrations below 8.5 cm.

The anion profiles at Sta. 37 (Fig. 1) were similar in shape to those at Sta. 35 with overlying values of approximately $450 \text{ mg Cl liter}^{-1}$, $5 \text{ mg Br liter}^{-1}$, and $75 \text{ mg SO}_4 \text{ liter}^{-1}$ to a depth of 3.5 cm followed by sharp increases in concentrations to a depth of 8.5 cm where the concentrations are $8,400 \text{ mg Cl liter}^{-1}$, $115 \text{ mg Br liter}^{-1}$, and $350 \text{ mg SO}_4 \text{ liter}^{-1}$. However, beneath that depth the concentrations of all the anions continued to increase to the bottom of the depth sampled (19.0 cm). The anion profiles at Sta. 30 (Fig. 1) were also similar in shape to those at Sta. 37, but the increase in concentrations began deeper at 5 cm with a sharp change in slope commencing at 8.5 cm.

Figure 2 shows the Cl/Br weight ratio with depth for the three profiles. The results from Stas. 35 and 37 showed constant Cl/Br ratios of 72 and 73 from 3.0 cm and 5.0 cm downward, respectively. Above these depths the Cl/Br ratio increased to values of ~ 80 at and somewhat above the sediment–water interface. At Sta. 30 the constant Cl/Br ratio beneath 8 cm was 69, somewhat lower than at the other two stations. The ratio above this depth increased more sharply, reaching values of >100 immediately at and above

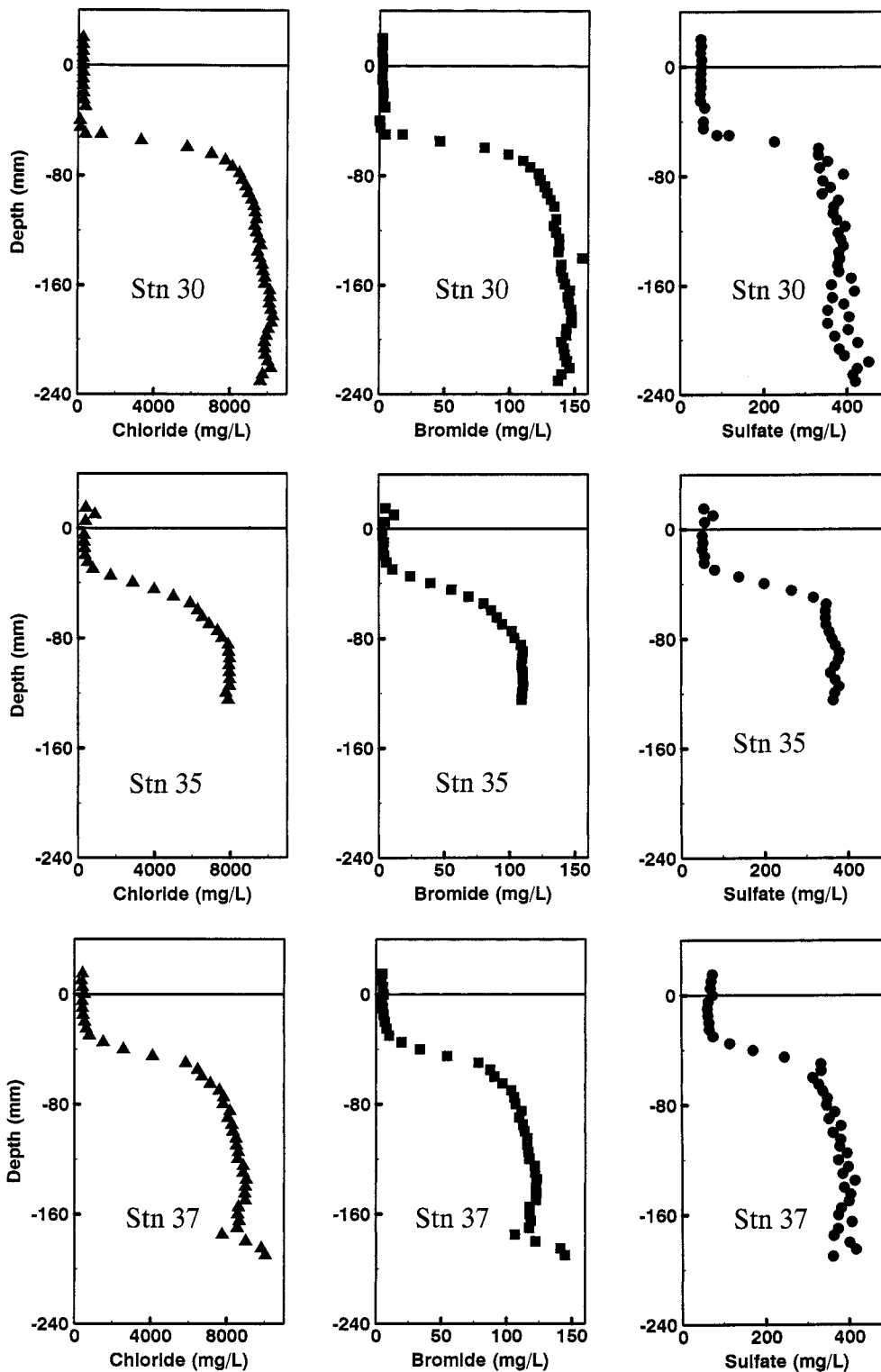


Fig. 1. Measured pore-water profiles of chloride, bromide, and sulfate at Stas. 30, 35, and 37.

the sediment–water interface. The measured composition of the THS was 17,340 mg Cl liter⁻¹, 237 mg Br liter⁻¹, and 727 mg SO₄ liter⁻¹ with a Cl/Br weight ratio of 73.1.

A seepage flux meter deployed off the THS in the approximate area of gel profile Sta. 35 measured an MSF of

97 cm yr⁻¹ for a porosity of 0.59 that gives a LIV of 164 cm yr⁻¹ (Table 2). A flux meter located near gel profile Sta. 30 measured an MSF of 18 cm yr⁻¹ and an LIV of 30 cm yr⁻¹ during the same time interval.

The pore-water profiles and seepage meter measurements

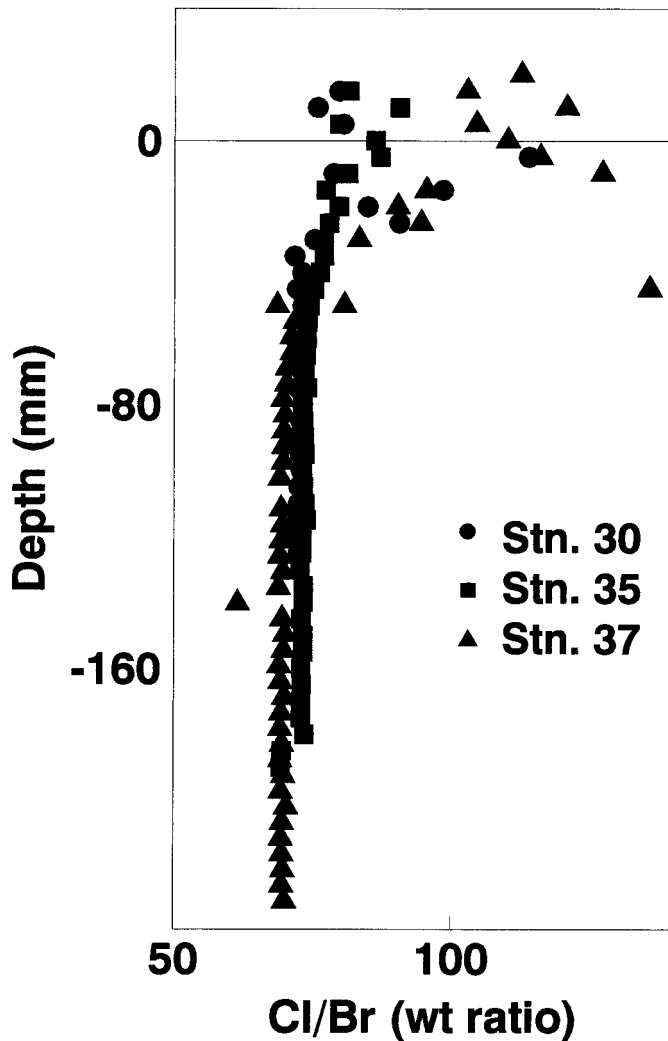


Fig. 2. Figure showing the Cl/Br ratio in the measured pore-water profiles at Stas. 30, 35, and 37.

obtained in this study suggest that this location represents an active area of saline groundwater seepage into the lake. Saline water with a composition of approximately 8,000 mg Cl liter⁻¹, 110 mg Br liter⁻¹, and 380 mg SO₄ liter⁻¹ occurred in the sediment interstitial waters from a depth of 8 cm downward. The composition of this saline water compared with that of the adjacent THS (17,340 mg Cl liter⁻¹, 237 mg Br liter⁻¹, and 727 mg SO₄ liter⁻¹) indicates a dilution of sediment pore waters by a factor of ~2 with the THS-type waters having been mixed with a freshwater source, possibly but not necessarily lake water. The pore waters of the upper layer of the sediment have a chemical composition (Table 1) that approaches that of lake water (225 mg Cl liter⁻¹, 2.2 mg Br liter⁻¹, and 50 mg SO₄ liter⁻¹; Nishri et al. 1997). Due to wave action and other turbulent mixing processes, the discharging groundwaters mix with the lake water into the sediment. Qualitative evidence for the relative magnitude of wave or turbulent mixing at these three stations is given by the depth at which the sharp gradient commences, which is deeper at Sta. 30 (5 cm) than at Stas. 35 or 37 (3–3.5 cm).

Table 2. Seepage rate measurements made at the Tiberias Hot Springs site, Lake Kinneret, Israel.

Seepage meter no.	Seepage rate	Seepage velocity (cm yr ⁻¹)	Linear interstitial velocity ($\phi = 0.59$; cm yr ⁻¹)	Remarks
TH35	2.66	97.0	164	Station 35 of the gel probe measurements
TH30	0.49	17.8	30	This meter was lost during a storm shortly after these measurements were taken

This suggests that the mixing energy at the shallower station (Sta. 30, 4.5 m depth) is greater than that at Stas. 35 (5.0 m) and 37 (5.5 m).

Modeling of pore-water profiles—The profiles of chloride, bromide, and sulfate were compared with calculated profiles produced by an advection–diffusion model. It was assumed for the model that the anion profiles were at steady state. The calculation was carried out using an analytical solution of Fick's 2nd law as proposed by Munk (1966).

$$C_z = \frac{(e^{Uz/D_s} - 1)}{(e^{Ud/D_s} - 1)} \cdot (C_d - C_o) + C_o \quad (1)$$

where C_z is the concentration of the ion at depth z (mg cm⁻³), U is the LIV—negative measured from the sediment–water interface downward (cm s⁻¹) and positive from the sediment, upward into the lake, z is depth from the sediment–water interface downward (cm), D_s is the sediment diffusion coefficient (cm² s⁻¹), d is the depth in the sediment at which the ion concentration is constant (cm), C_d is the constant ionic concentration in the sediment at depth d (mg cm⁻³), and C_o is the pore-water concentration at the sediment surface (mg cm⁻³).

In order to use the analytical solution of the advection–diffusion model (Eq. 1), it was necessary to define appropriate boundary conditions as follows: (1) there was a fixed concentration of anions (C_o) close to the sediment–water interface. It appears that lake water is moving into the coarse sediment down to a few centimeters depth. The upper boundary was thus taken as the deepest point in the sediment where the concentration of ions is the same as that in the overlying lake water (Table 1). This occurred at 3 cm depth in the sediments at Sta. 35, 3.5 cm at Sta. 37, and 4.8 cm at Sta. 30. (2) The depth d and the concentration at that depth, C_d , was taken from the pore-water profiles and was the depth where the change in concentration with depth decreased to almost zero (8.5–10 cm; Table 1). (3) To use Eq. 1, it is necessary to have a suitable value for D_s , the sediment diffusion coefficient, because self diffusion of ions in pore waters is hindered by the sediment. The in-situ temperature of the lake in late November when the sampling was carried out was 18°C. Subsequent measurements made at the seep site have shown that although the saline water that is up-

welling originates from or is associated with the THS, the temperature in the upper 10–20 cm of the sediment is similar to that of the overlying water (A. Nishri unpubl. data). Thus, we have used values from Li and Gregory (1974) for the anionic diffusion coefficients at infinite dilution and 18°C.

In order to convert the diffusion coefficient at infinite dilution to a sediment diffusion coefficient, the following equation was used from Krom and Berner (1980).

$$\frac{D_o}{D_s} = \phi \cdot F \quad (2)$$

where D_s is the sediment diffusion coefficient, D_o is the diffusion coefficient at infinite dilution, F is the formation factor, and ϕ is the porosity.

A measured value of 0.59 (water content = 34%) was used for sediment porosity. Archie's factor (Manheim 1970) was then used to estimate the formation factor ($F = \phi^{-2}$). Substituting into Eq. 2 and simplifying results in:

$$D_s = \phi \cdot D_o \quad (3)$$

A spreadsheet program was created that included the measured pore-water depth profile and the calculated values of anion and concentration (C_z) at depth (z) for a given value of advection (U). The initial values of C_o , C_d , and d (Eq. 1) were taken from Fig. 1. The value of U was then altered by $\pm 10\%$ until the best fit to the measured profile of chloride was obtained using a least-squares fit procedure. It was found, however, that with minor adjustments to the values of C_o , C_d , and d to those given in Table 1, a modified value of U resulted in the lowest value for the least-squares fit. For each value of this best-fit value of U , values for $U \cdot 2$ and $U/2$ were calculated at the same time to show the sensitivity of the procedure (Fig. 3). The final best-fit values obtained involved using data with the maximum concentration gradient. This suggested that there had been a minor relaxation of the concentration of chloride (and other ions) at the upper and lower boundaries (~ 1 cm) between the time the probe was removed from the sediment and the time it was sectioned. The best-fit values of U and z calculated in this manner for chloride were then used to generate modeled profiles for bromide and sulfate. In all cases, it was found that the best fit obtained for chloride was also the best fit for bromide and close to the best fit for sulfate.

Figure 3 shows the modeled pore-water profiles of chloride, bromide, and sulfate with depth together with the measured interstitial profiles for all three stations. In order to give some feel for sensitivity of the best fit to different values of the linear advection velocity (U), the curves obtained for $U/2$ and $U \cdot 2$ are plotted also in Fig. 3. Based on this procedure, the value for U (and hence LIV) for each station could be discriminated to $\pm 25\%$ or better. The linear interstitial velocity (cm yr^{-1}), initial concentration (C_o , mg liter^{-1}), concentration at depth (C_d , mg liter^{-1}), and the depths where the sharp concentration gradient started and ceased are given in Table 1.

Between 3.0 and 8.5 cm in the sediments there were steep chemical gradients in all three locations of approximately 1,250 ppm Cl cm^{-1} , 15.4 ppm Br cm^{-1} , and 50 ppm SO_4 cm^{-1} . The quality of the fits of the modeled curves of chloride and bromide to the measured data shows that the as-

sumptions involved in the advection–diffusion model are valid. Although the effective diffusion coefficient of sulfate is approximately half that of chloride and bromide, the modeled curve using the same value of advection rate and boundary conditions also fits well to the measured sulfate data. There was, however, evidence for some minor nonconservative behavior in the sulfate profiles. In the normal muddy sediments of the lake, sulfate is often entirely removed in the upper few centimeters as a result of microbial sulfate reduction (Hadas and Pinkas 1995). In the sandy littoral area of the Tiberias underwater seeps some biological remediation of sulfate can be expected.

An assumption of the simple analytical solution to Fick's 2nd law used in this study is that the porosity remains constant with depth over the depth interval where the concentration changes. It was not possible to obtain a sediment core at this location to determine directly the porosity profile with depth. However, a core was obtained from a location close to the 30-m site but in somewhat shallower water. This core showed no systematic change in porosity with depth with a variability of less than ± 0.1 porosity units. Figure 4 shows that differences in modeled profiles obtained for a change in porosity of ± 0.1 units have little effect on the calculated LIV. Furthermore in locations where porosity has been shown to vary systematically with depth, by far the largest changes occur over the upper 1–2 cm (Andrews and Bennett 1981). In this system the major anion gradient and the modeling depth was from 3 to 8 cm in the core.

Andrews and Bennett (1981) have suggested that in certain types of sediment, ϕ^{-3} is a better representation of Archie's factor than the ϕ^{-2} . Their data suggest that a value of $\phi^{-2.1}$ is appropriate for sandy sediments increasing to ϕ^{-3} in fine muds. Thus, although it is most appropriate to use ϕ^{-2} in this study, we have also calculated our D_s values using an Archie's factor of ϕ^{-3} as a measure of sensitivity. This resulted in a decrease of $\sim 35\text{--}40\%$ in the LIV, with the values being 160, 90, and 120 cm yr^{-1} for Stas. 30, 35, and 37, respectively.

The linear advection velocities measured by the seepage meters at Stas. 30 and 35 were 30 and 164 cm yr^{-1} , respectively. These values represent 12% and 109% of the modeled gel profile values for these stations. There are a number of possible reasons as to why these two methods agree within error for Sta. 35 but not for Sta. 30. Generally, for littoral seepage work, seepage meters have efficiency factors of 60–80%. For Sta. 30 the results are so far apart that this efficiency factor cannot be the only reason causing discrepancies in the two methods. A number of workers (Lee 1977; Shaw and Prepas 1990; and references therein) have shown that seepage in the littoral zones of lakes can be quite heterogeneous, both spatially and temporally. Furthermore the flux meter measures an area of 0.322 m^2 , whereas the gel profiler occupies an area less than 0.002 m^2 . Thus seepage heterogeneity is probably the main factor causing the large discrepancy in flux rates at Sta. 30. Seepage measurement at an adjacent site was ~ 25 cm yr^{-1} (Dror and Stiller unpubl. data). At this time, neither of these methods can be considered to measure absolute seepage fluxes; to do so would require extensive simultaneous calibration of both systems under standardized known flow conditions.

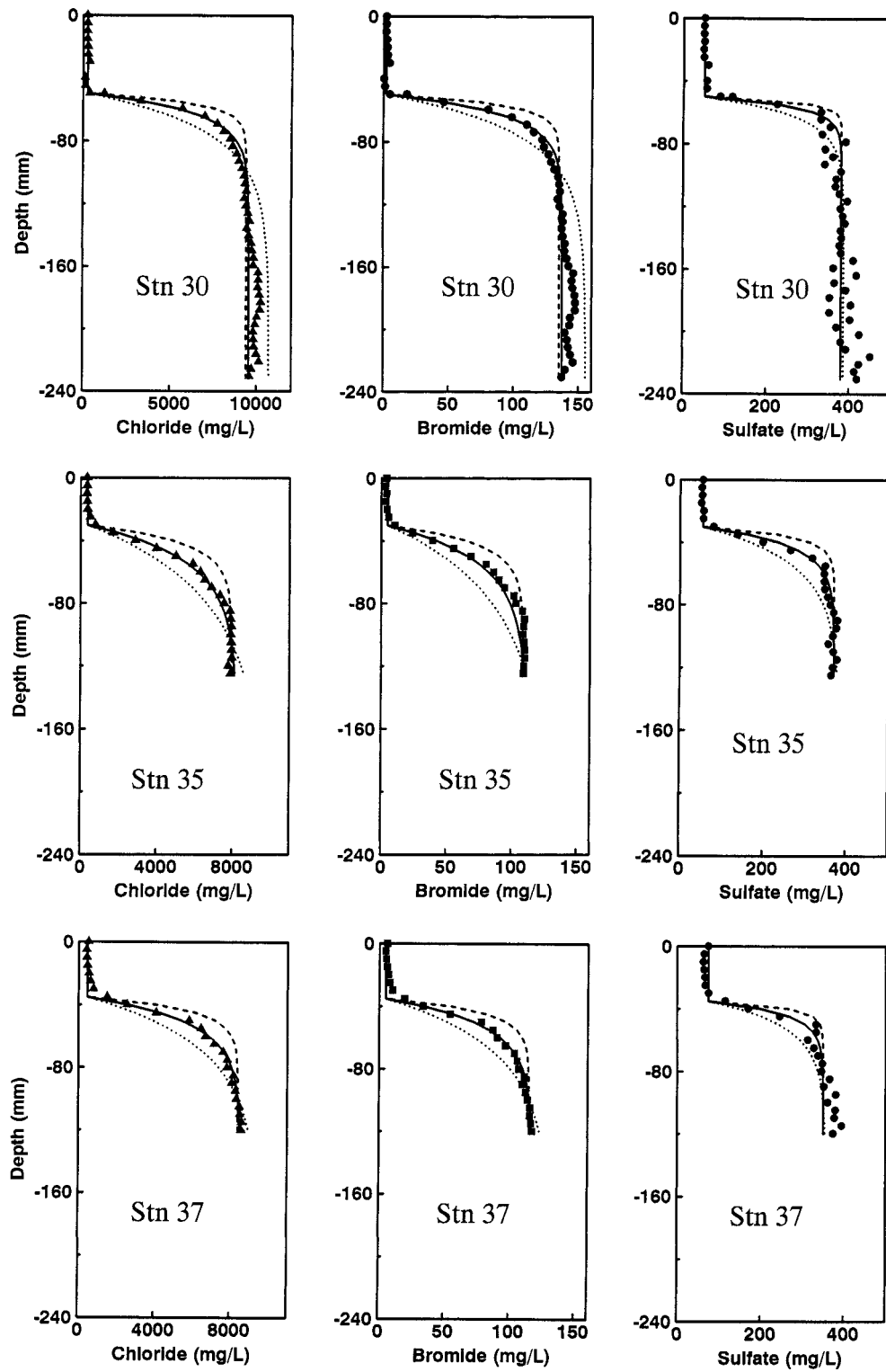


Fig. 3. Best-fit modeled pore-water profile at Stas. 30, 35, and 37 for the values of U given in Table 1, together with the profile obtained by using $U/2$ and $U \cdot 2$, compared with the measured profiles for chloride, bromide, and sulfate.

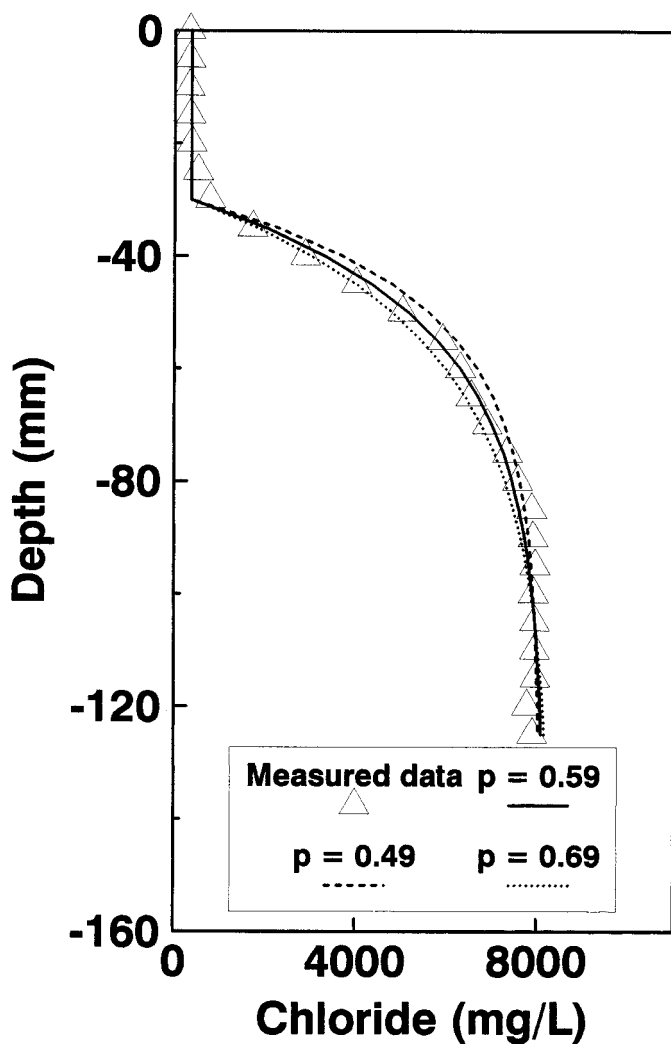


Fig. 4. Sensitivity of the advection-diffusion model to changes in porosity of ± 0.1 porosity units from the measured value.

Smith et al. (1989) have calculated that the total influx of chloride to the lake from internal sources is 90,000 tones. Stiller (1994) estimated that approximately 10% of this input is derived from chloride that diffuses into the lake via the muddy sediment found at water depths greater than 23 m throughout the lake. In order to estimate the importance of the THS seepage (and other similar seeps) to the overall chloride budget of the lake, a simple flux calculation was carried out. The average measured advective flux of 250 cm yr^{-1} corresponds to a water flux of 6.8 liters $\text{m}^{-2} \text{d}^{-1}$ or 2,500 liters $\text{m}^{-2} \text{yr}^{-1}$. Each liter of this saline seep contains 8 g Cl liter $^{-1}$ ($\sim 8,000$ mg liter $^{-1}$). Therefore, the input of chloride to the lake is 20 kg Cl $\text{m}^{-2} \text{yr}^{-1}$. At present we do not know the area affected by this particular seep. A conservative estimate might be 40 m \times 30 m (1,200 m^2), which corresponds to a total input of 24 tones of chloride per year. Alternatively, the area of seepage required to contribute 81,000 tones of chloride per year at the flux rate determined in this study would be 4 km^2 . It seems unlikely that there is such a large

area of saline seeps in the bottom of the lake. This suggests that saline springs that input water directly into the lake are probably the major point source of salt to the lake.

Both the gel profiling and seepage flux meter systems were used to estimate groundwater seepage fluxes in the littoral environment of the THS site. The gel profiler system, which was used for the first time in this study, displays excellent potential as a littoral groundwater seepage measurement system, especially in sandy lake sediments that cannot be sampled easily using conventional methods. Provided there is sufficient contrast between the chemical composition of lake column and sediment pore waters, the gel profiler has good application also in the nonlittoral portions of lakes. The present research demonstrates some of the advantages, disadvantages, and discrepancies in using physical (flux meters) and chemical modeling (gel profile) methods of measuring littoral lake seepage fluxes.

R. J. G. Mortimer
M. D. Krom

School of Earth Sciences
University of Leeds, Leeds
West Yorkshire LS2 9JT, United Kingdom

D. R. Boyle

Geological Survey of Canada
601 Booth St., Ottawa
Ontario K1A 0E8, Canada

A. Nishri

I.O.L.R., Kinneret Limnological Laboratory
Tiberias, POB 345, Israel

References

- ANDREWS, D., AND A. BENNETT. 1981. Measurements of diffusivity near the sediment-water interface with a fine-scale resistivity probe. *Geochim. Cosmochim. Acta* **45**: 2169-2175.
- BERNER, R. A. 1972. *Principles of chemical sedimentology*. McGraw-Hill.
- BOYLE, D. R. 1994. Design of a seepage meter for measuring groundwater fluxes in the nonlittoral zones of lakes—evaluation in a boreal forest lake. *Limnol. Oceanogr.* **39**: 670-681.
- CHERKAUER, D. S., AND J. M. McBRIDE. 1988. A remotely operated seepage meter for use in large lakes and rivers. *Groundwater* **26**: 165-171.
- CORNETT, R. J., B. A. RISTO, AND D. R. LEE. 1989. Measuring groundwater transport through lake sediments by advection and diffusion. *Water Resources Res.* **25**: 1815-1823.
- ERICKSON, D. R. 1981. A study of littoral groundwater seepage at Williams Lake, Minnesota using seepage meters and wells. M.S. thesis, Univ. Minnesota.
- HADAS, O., AND R. PINKAS. 1995. Sulfate reduction in the hypolim-

Acknowledgments

This work was funded by the Israel Water Commission. We thank Mira Stiller for the long and detailed discussions that greatly helped to crystallize our thoughts on this study. The development work on the gel probes used in this study were funded by NERC grants GST/02/753 and GR9/1320. A travel grant for R.J.G.M. to visit Israel was provided by the British Council and by the Anglo-Israel Academic fund.

- nion and sediments of Lake Kinneret, Israel. *Freshwater Biol.* **33**: 63–72.
- KRABBEHOFT, D. P., C. C. GILMOUR, J. M. BENOIT, C. L. BABIARZ, A. W. ANDREN, AND J. P. HURLEY. 1998. Methyl mercury dynamics in littoral sediments of a temperate seepage lake. *Can. J. Fish. Aquat. Sci.* **55**: 835–844.
- KROM, M. D., AND R. A. BERNER. 1980. The diffusion coefficients of sulfate, ammonium and phosphate in anoxic marine sediments. *Limnol. Oceanogr.* **25**: 327–337.
- , P. DAVISON, H. ZHANG, AND W. DAVISON. 1994. High resolution pore water sampling using a gel sampler. *Limnol. Oceanogr.* **39**: 1967–1972.
- LEE, D. R. 1977. A device for measuring seepage flux in lakes and estuaries. *Limnol. Oceanogr.* **22**: 140–147.
- , AND J. A. CHERRY. 1978. A field exercise on groundwater flow using seepage meters and mini-piezometers. *J. Geol. Educ.* **27**: 610.
- , ———, AND J. F. PICKENS. 1980. Groundwater transport of a salt tracer through a sandy lakebed. *Limnol. Oceanogr.* **25**: 45–61.
- LI, Y.-H., AND S. GREGORY. 1974. Diffusion of ions in seawater and in deep-sea sediments. *Geochim. Cosmochim. Acta* **38**: 703–714.
- MANHEIM, F. T. 1970. The diffusion of ions in unconsolidated sediments. *Earth Planet. Sci. Lett.* **9**: 307–309.
- MANWARING, C. E. 1996. Measurements of salinity gradients in the bottom sediments of Lake Kinneret, using gel and conventional porewater sampling, Israel. M.Sc. thesis, Leeds Univ.
- MORTIMER, R. J. G., M. D. KROM, P. O. J. HALL, S. HULTH, AND H. STÄHL. 1998. Use of gel probes for the determination of high resolution solute distributions in marine and estuarine pore waters. *Mar. Chem.* **63**: 119–129.
- MUNK, W. H. 1966. Abyssal recipes. *Deep Sea Res.* **13**: 707–730.
- NISHRI, A., M. STILLER, A. RIMMER, Y. GEIFMAN, AND M. D. KROM. (1999) Lake Kinneret (The Sea of Galilee): The effects of diversion of external salinity sources and the probable chemical composition of the internal salinity sources. *Chem. Geol.* **158**: 37–52.
- , ———, AND D. RONEN. 1997. Comparison between methods for estimating un-focused seepage from Lake Kinneret bed sediments. IOLR report T14/97.
- SHAW, R. D., AND E. E. PREPAS. 1990. Groundwater–lake interactions: I. Accuracy of seepage meter estimates of lake seepage. *J. Hydrol.* **119**: 105–120.
- SMITH, S. V., S. SERRUYA, Y. GEIFMAN, AND T. BERMAN. 1989. Internal sources and sinks of water, P, N, Ca, and Cl in Lake Kinneret, Israel. *Limnol. Oceanogr.* **34**: 1202–1213.
- STILLER, M. 1994. The chloride content in pore water of Lake Kinneret sediments. *Isr. J. Earth Sci.* **43**: 179–185.

Received: 26 May 1998

Accepted: 14 June 1999

Amended: 30 June 1999

Linking diagenetic alteration of amino acids and bulk organic matter reactivity

Abstract—Examination of amino acids in particulate samples from a variety of marine environments (fresh phytoplankton to deep-sea sediments) revealed systematic compositional changes upon progressive degradation. These consistent trends have been used to derive a quantitative degradation index (DI) that is directly related to the reactivity of the organic material, as indicated by its lability to enzymatic decay and its first-order degradation rate constant. This direct link between molecular composition and degradation rate allows us to quantify the quality of organic matter based solely on its chemical composition.

Decomposition of particulate organic matter (POM) is responsible for oxygen consumption in the ocean and its sediments, for the recycling of essential nutrients, and for most early diagenetic processes. The heterogeneous composition of POM leads to selective preservation of more stable (or less available) molecular compounds and to the loss of labile compounds, resulting in a continuously altered biochemical composition of the material during diagenesis (Tegelaar et al. 1989; Cowie and Hedges 1994; Wakeham et al. 1997). These compositional changes in POM are probably the reason for a decreasing first-order degradation rate (Middelburg 1989) and a reduced nutritional value toward heterotrophic consumers (Tenore et al. 1984) as degradation proceeds. Although intrinsic differences in molecular structure (de Leeuw

and Largeau 1993) and differences in physiochemical association with the sediment matrix (Keil et al. 1994; Mayer 1994) are documented factors acting on early diagenesis of POM, there are few studies that directly link the resulting shifts in biochemical composition to the degradation state (Cowie and Hedges 1994; Wakeham et al. 1997; Dauwe and Middelburg 1998). Moreover, compositional characteristics of organic matter have not yet been linked to its biological availability or its degradation dynamics.

A series of molecular diagenetic maturity indicators have been used to estimate the relative degradation state of the organic matter (Cowie and Hedges 1994; Wakeham et al. 1997), varying from short-term (e.g., chlorophyll) to longer term (e.g., nonprotein amino acids) indicators. Broadly applicable degradation state indicators should be based on major components that are widely distributed geographically and that are omnipresent in organisms so that variability in sources of organic matter is minimized. Moreover, they should ideally be sensitive to all stages of alteration. Proteins are ubiquitous components of all source organisms and degradation mixtures (Cowie and Hedges 1992). Although there is some dissimilarity in amino acid composition of the ultimate source organisms (e.g., diatoms, coccolithophorids, and bacteria) (Cowie and Hedges 1992), these differences are minor compared to the alteration of the spectra upon degradation (Dauwe and Middelburg 1998).